Inorganica Chimica Acta 387 (2012) 441–445

Contents lists available at SciVerse ScienceDirect

Inorganica Chimica Acta

journal homepage: www.elsevier.com/locate/ica

Note

Palladium(II) complexes of tridentate chalcogenated Schiff bases and related ligands of (S, N, S/Se/Te) type: Synthesis and structural chemistry

Pradhumn Singh, Ajai K. Singh *

Department of Chemistry, Indian Institute of Technology Delhi, New Delhi 110016, India

A R T I C L E I N F O

Article history:
Received 4 September 2011
Received in revised form 5 December 2011
Accepted 4 January 2012
Available online 10 January 2012

Keywords:
Organochalcogen ligand
Schiff base
Secondary amine
Palladium(II)
Synthesis
Crystal structure

A B S T R A C T

The reactions in CH_3CN between $PdCl_2$ and Schiff base ligands, 2-$MeSC_6H_4$–CH=NCH_2CH_2E–C_6H_4–4-R (**L1–L3**) (E = S or Se, R = H; E = Te, R = OCH_3) and their reduced derivatives 2-$MeSC_6H_4CH_2$–$NHCH_2CH_2E$–C_6H_4–4-R (**L4–L6**) followed by treatment with $AgPF_6$ or $AgClO_4$ have resulted in complexes [PdCl(**L**)][X] (**1–6; L** = **L1–L6**; X = PF_6 or ClO_4) which have been characterized by IR, ^1H, $^{13}C\{^1H\}$, $^{77}Se\{^1H\}$ and $^{125}Te\{^1H\}$ NMR spectroscopy. Single crystal structures of complexes **1–6** reveal nearly square planar geometry around palladium in all of them (Pd–Se = 2.4045(16)–2.4065(6) Å; Pd–Te = 2.5052(9)–2.5307(13) Å). The various non-covalent interactions in the crystals result in the formation of chains, rings and caging of anions between cations.

1. Introduction

Chalcogenated Schiff bases containing both 'soft' and 'hard' donor sites are hybrid ligands which may show hemilabile behavior. Thus they are not only academic curiosities but also attractive for catalyst designing as facile reversible generation of a coordinatively unsaturated metal center [1] is possible in their metal complexes. In the recent past catalytic applications of Pd(II)-complexes of sulfated [2–5], selenated [5,6] and tellurated Schiff bases [7,8] have been reported. Among chalcogenated Schiff bases those containing thioether donor site have been explored more than selenated and tellurated ones. In fact selenated and tellurated ones are still scarcely known.

The secondary amines synthesized from Schiff bases by reduction of their >C=N bond are stable and more adaptable to form conformationally flexible five- or six-membered rings on complexation with metal ions than their precursors, which are constrained to be planar. The hydrogen of their >NH formed due to reduction of azomethine group of Schiff base becomes significantly better acidic on coordination of N to a metal ion. Consequently coordinated N–H may better participate in intermolecular hydrogen-bonding, resulting in the supramolecular self-assembly of their metal complexes [9]. There are many examples of their metal complexes in literature [9–11]. Some of them have N, O and P donor sites but only few of them have chalcogen donor atoms, particularly selenium or tellurium [4,12,13]. Copper complexes of reduced Schiff bases prepared from salicylaldehyde and amino acids were explored as models for intermediate species in biological racemization and transamination reactions [10]. Recently Rao et al. [14] have reported an air and moisture insensitive palladacycle [PdCl(**L**–H)], where **L** = (N, Se, C^-) ligand $(C_6H_5)(2\text{-}HOC_6H_4)CHNH(CH_2)_3SePh$. This palladacycle shows high catalytic activity for Suzuki–Miyaura coupling reaction of phenylboronic acid with aryl/heteroaryl chlorides/bromides (TON for ArCl up to 9200) and is converted to ~8 nm size nanoparticles of composition $Pd_{17}Se_{15}$, which have been proposed to be the real catalysts. It was therefore thought worthwhile to study ligation of **L** (**L1–L6**; Scheme 1) with palladium(II). Thus complexes, [PdCl(**L**)][PF_6/ClO_4] of tridentate Schiff bases 2-$MeSC_6H_4$CH=NCH_2 CH_2E–C_6H_4–4-R (**L1–L3**) and their reduced derivatives 2-$MeSC_6$ H_4CH_2–$NHCH_2CH_2E$–C_6H_4–4-R (**L4–L6**) (where E = S or Se, R = H; E = Te, R = OCH_3) were synthesized and explored for their structural chemistry. The crystal structures of these complexes have a variety of non-covalent interactions, which result in interesting structural patterns. These results are given in the present paper.

2. Experimental

2.1. Physical measurement

Perkin-Elmer 2400 Series II C, H, N analyzer was used for elemental analyses. The ^1H, $^{13}C\{^1H\}$, $^{77}Se\{^1H\}$ and $^{125}Te\{^1H\}$ NMR spectra were recorded on a Bruker Spectrospin DPX–300 NMR

---

* Corresponding author. Tel.: +91 11 26591379; fax: +91 11 26581102.
E-mail addresses: aksingh@chemistry.iitd.ac.in, ajai57@hotmail.com (A.K. Singh).

0020-1693/$ - see front matter © 2012 Elsevier B.V. All rights reserved.
doi:10.1016/j.ica.2012.01.007

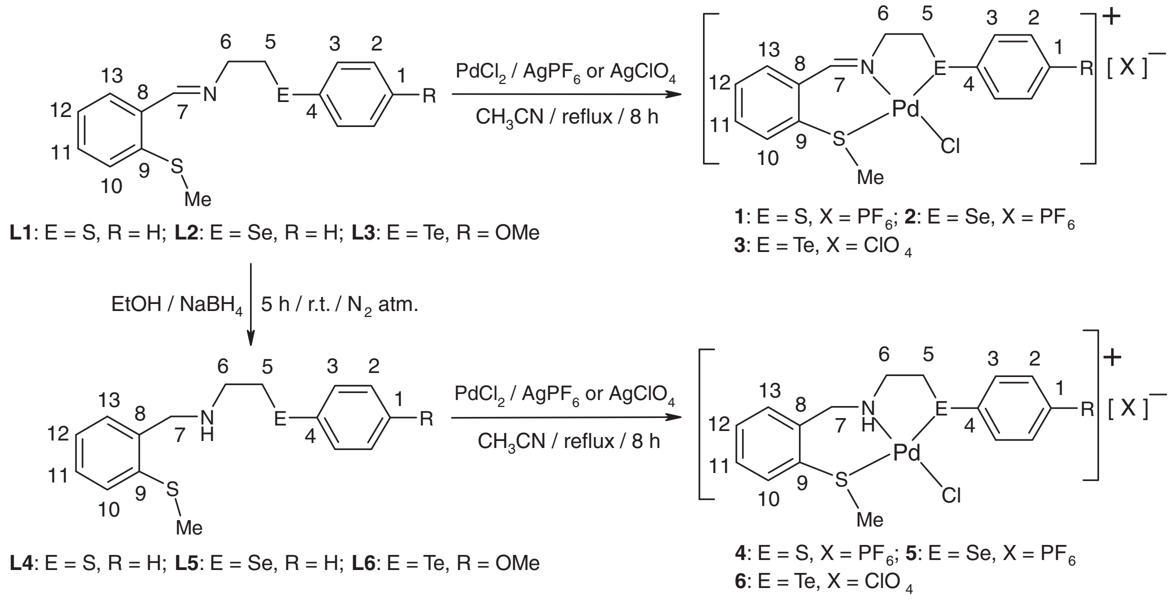

Scheme 1. Syntheses of Pd(II)–complexes **1–6**.

spectrometer at 300.13, 75.47, 57.24 and 94.69 MHz, respectively. IR spectra in the range 4000–400 cm^{-1} were recorded on a Nicolet Protége 460 FT-IR spectrometer. The diffraction data on single-crystals of **1–6** were collected on a Bruker AXS SMART Apex CCD diffractometer using Mo Kα (0.71073 Å) radiations at 298(2) K. The software SADABS [15] was used for absorption correction (if needed) and SHELXTL for space group, structure determination and refinements [16]. All non-hydrogen atoms were refined anisotropically. Hydrogen atoms were included in idealized positions with isotropic thermal parameters set at 1.2 times that of the carbon atom to which they are attached. The least-square refinement cycles on F^2 were performed until the model converged. The conductivity measurements were made in CH_3CN (Concentration ca. 1 mM) using ORION conductivity meter model 162. Melting points determined in open capillary are reported as such.

2.2. Chemicals and reagents

2-(Phenylsulfanyl)ethylamine, 2-(phenylseleno)ethylamine and 2-(4-methoxyphenyltelluro)ethylamine were synthesized by reported methods [17–20]. 2-(Methylthio)benzaldehyde, $PdCl_2$, $AgPF_6$ and $AgClO_4$ were procured from Sigma–Aldrich (USA) and used as received. All the solvents were dried and distilled before use by standard procedures [21]. The **L1**–**L6** have been synthesized according to procedure reported earlier by us [22,23].

2.3. Synthesis of palladium(II) complexes (*1*–*6*)

The CH_3CN (20 cm^3) and solid $PdCl_2$ (0.18 g, 1 mmol) were mixed and the mixture was refluxed with stirring until a clear light yellow coloured solution was obtained. The solution of a ligand from **L1** to **L6** (0.28–0.42 g, 1 mmol) made in CH_3OH (5 cm^3) was added to it and the mixture refluxed for 5 h. Thereafter $AgPF_6$ (0.25 g, 1 mmol)/$AgClO_4$ (0.21 g, 1 mmol) was mixed and the mixture further refluxed for 3 h. It was cooled to room temperature and turbidity of AgCl was filtered off. The filtrate was concentrated to ~5 cm^3 on a rotary evaporator and mixed with diethyl ether (10 cm^3) to obtain **1–6** as yellow-orange solid, which was filtered and dried *in vacuo*. The single crystals of **1–6** were grown by slow evaporation of their solutions in CH_3CN–CH_3OH mixture (3:2).

Caution: Perchlorate is potentially explosive and therefore should be handled carefully.

*Complex **1**:* Yellow solid. Yield: 0.49 g, 85%; m.p. 152 °C. Λ_M = 148.4 S cm^2 mol^{-1}. *Anal.* Calc. for $C_{16}H_{17}ClNPdS_2{\cdot}PF_6$: C, 33.47; H, 2.98; N, 2.44. Found: C, 33.41; H, 2.91; N, 2.49%. ^{1}H NMR (CD_3CN, 25 °C, versus Me_4Si): (δ, ppm): 2.99 (s, 3H, SCH_3), 3.23–3.27 (m, 2H, H_5), 4.26–4.30 (m, 2H, H_6), 7.53–8.09 (m, 9H, H_{1-3}, H_{10-13}), 8.52 (s, 1H, H_7). $^{13}C\{^1H\}$ NMR (CD_3CN, 25 °C, versus Me_4Si): (δ, ppm): 27.9 (SCH_3), 39.5 (C_5), 70.3 (C_6), 125.2–134.3 (C_{1-4}, C_{10-13}), 137.3 (C_8), 139.8 (C_9), 166.9 (C_7). IR (KBr, ν_{max}/cm^{-1}): 3055 (m; $\nu_{C-H(aromatic)}$), 2920 (s; $\nu_{C-H(aliphatic)}$), 1634, 1580 (s; $\nu_{C=N}$), 1225 (m; ν_{C-N}), 838 (s; ν_{P-F}), 748 (m; $\nu_{C-H(aromatic)}$).

*Complex **2***: Orange solid. Yield: 0.53 g, 85%; m.p. 148.0 °C. Λ_M = 145.8 S cm^2 mol^{-1}. *Anal.* Calc. for $C_{16}H_{17}ClNPdSSe{\cdot}PF_6$: C, 30.94; H, 2.76; N, 2.26. Found: C, 30.89; H, 2.70; N, 2.20%. ^{1}H NMR (CD_3CN, 25 °C, versus Me_4Si): (δ, ppm): 3.00 (s, 3H, SCH_3), 3.05–3.25 (m, 2H, H_5), 4.35–4.81 (m, 2H, H_6), 7.54–8.12 (m, 9H, H_{1-3}, H_{10-13}), 8.50 (s, 1H, H_7). $^{13}C\{^1H\}$ NMR (CD_3CN, 25 °C, versus Me_4Si): (δ, ppm): 26.0 (SCH_3), 32.5 (C_5), 72.1 (C_6), 126.2–134.6 (C_{1-4}, C_{10-13}), 137.0 (C_8), 139.4 (C_9), 167.5 (C_7). $^{77}Se\{^1H\}$ NMR (CD_3CN, 25 °C, versus Me_2Se): (δ, ppm): 456.2. IR (KBr, ν_{max}/cm^{-1}): 3055 (m; $\nu_{C-H(aromatic)}$), 2919 (s; $\nu_{C-H(aliphatic)}$), 1632, 1579 (s; $\nu_{C=N}$), 1191 (m; ν_{C-N}), 839 (m; ν_{P-F}), 745 (m; $\nu_{C-H(aromatic)}$).

*Complex **3***: Orange solid. Yield: 0.56 g, 85%; m.p. 147.0 °C. Λ_M = 142.3 S cm^2 mol^{-1}. *Anal.* Calc. for $C_{17}H_{19}ClNOPdSTe{\cdot}ClO_4$: C, 31.11; H, 3.22; N, 2.13. Found: C, 31.02; H, 3.17; N, 2.19%. ^{1}H NMR (CD_3CN, 25 °C, versus Me_4Si): (δ, ppm): 2.50–2.90 (m, 2H, H_5), 2.97 (s, 3H, SCH_3), 3.85 (s, 3H, OCH_3), 4.83–5.74 (m, 2H, H_6), 7.05 (d, $^3J_{H-H}$ = 8.7 Hz, 2H, H_2), 7.36–7.93 (m, 4H, H_{10-13}), 7.99 (d, $^3J_{H-H}$ = 8.7 Hz, 2H, H_3), 8.46 (s, 1H, H_7). $^{13}C\{^1H\}$ NMR (CD_3CN, 25 °C, versus Me_4Si): (δ, ppm): 17.0 (C_5), 21.9 (SCH_3), 56.3 (OCH_3), 74.5 (C_6), 105.6 (C_4), 117.2 (C_2), 128.5–134.0 (C_{10-13}), 136.4(C_8), 138.5 (C_9), 139.6 (C_3), 163.0 (C_1), 168.8 (C_7). $^{125}Te\{^1H\}$ NMR (CD_3CN, 25 °C, versus Me_2Te): (δ, ppm): 792.2. IR (KBr, ν_{max}/cm^{-1}): 3048 (m; $\nu_{C-H(aromatic)}$), 2926 (s; $\nu_{C-H(aliphatic)}$), 1632, 1583 (s; $\nu_{C=N}$), 1201 (m; ν_{C-N}), 747 (m; $\nu_{C-H(aromatic)}$).

*Complex **4***: Yellow solid. Yield: 0.49 g, 85%; m.p. 157.0 °C. Λ_M = 137.8 S cm^2 mol^{-1}. *Anal.* Calc. for $C_{16}H_{19}ClNPdS_2{\cdot}PF_6$: C, 33.35; H, 3.32; N, 2.43. Found: C, 33.30; H, 3.38; N, 2.49%. ^{1}H NMR (CD_3CN, 25 °C, versus Me_4Si): (δ, ppm): 2.09 (s, 1H, NH), 2.91 (s, 3H, SCH_3), 3.38–3.94 (m, 2H, H_5), 4.44–4.95 (m, 2H, H_6), 5.13 (s, 2H, H_7), 7.53–7.77 (m, 8H, H_{1-2}, H_{10-13}), 8.02–8.09 (m, 2H, H_3). $^{13}C\{^1H\}$ NMR (CD_3CN, 25 °C, versus Me_4Si): (δ, ppm): 23.3 (SCH_3), 40.5 (C_5), 56.8 (C_6), 62.6 (C_7), 126.9–137.2 (C_{1-4}, C_{10-13}). IR (KBr, ν_{max}/cm^{-1}): 3049 (m; $\nu_{C-H(aromatic)}$), 2922 (s; $\nu_{C-H(aliphatic)}$), 1181 (m; ν_{C-N}), 742 (m; $\nu_{C-H(aromatic)}$).

*Complex **5***: Orange solid. Yield: 0.53 g, 85%; m.p. 152.0 °C. $\Lambda_M = 135.6\ S\ cm^2\ mol^{-1}$. *Anal.* Calc. for $C_{16}H_{19}ClNPdSSe{\cdot}PF_6$: C, 30.84; H, 3.07; N, 2.25. Found: C, 30.80; H, 3.01; N, 2.20%. ^1H NMR (CD_3CN, 25 °C, versus Me_4Si): (δ, ppm): 2.19 (s, 1H, NH), 2.94 (s, 3H, SCH_3), 3.32–3.92 (m, 2H, H_5), 4.32–4.63 (m, 2H, H_6), 5.00 (s, 2H, H_7), 7.53–7.88 (m, 8H, H_{1-2}, H_{10-13}), 8.02–8.10 (m, 2H, H_3). $^{13}C\{^1H\}$ NMR (CD_3CN, 25 °C, versus Me_4Si): (δ, ppm): 21.5 (SCH_3), 33.0 (C_5), 56.1 (C_6), 60.0 (C_7), 126.6–136.6 (C_{1-4}, C_{10-13}). $^{77}Se\{^1H\}$ NMR (CD_3CN, 25 °C, versus Me_2Se): (δ, ppm): 429.5. IR (KBr, ν_{max}/cm^{-1}): 3049 (m; $\nu_{C-H(aromatic)}$), 2924 (s; $\nu_{C-H(aliphatic)}$), 1179 (m; ν_{C-N}), 741 (m; $\nu_{C-H(aromatic)}$).

*Complex **6***: Orange solid. Yield: 0.60 g, 85%; m.p. 154.2 °C. $\Lambda_M = 134.2\ S\ cm^2\ mol^{-1}$. *Anal.* Calc. for $C_{17}H_{21}ClNOPdSTe{\cdot}ClO_4$: C, 31.11; H, 3.22; N, 2.13. Found: C, 31.18; H, 3.20; N, 2.18%. ^1H NMR (CD_3CN, 25 °C, versus Me_4Si): (δ, ppm): 2.19 (1H, s, NH), 2.90 (s, 3H, SCH_3), 3.02–3.70 (m, 2H, H_5), 3.85 (s, 3H, OCH_3), 4.03–4.21 (m, 2H, H_6), 4.91 (s, 2H, H_7), 7.02 (d, 2H, $^3J_{H-H} = 7.5$ Hz, H_2), 7.49–7.63 (m, 4H, H_{10-13}), 7.89 (d, 2H, $^3J_{H-H} = 7.5$ Hz, H_3). $^{13}C\{^1H\}$ NMR (CD_3CN, 25 °C, versus Me_4Si): (δ, ppm): 16.7 (C_5), 18.6 (SCH_3), 56.2 (C_6), 56.5 (OCH_3), 61.2 (C_7), 105.7 (C_4), 116.9 (C_2), 126.2–133.4 (C_{10-13}), 135.5 (C_8), 137.2 (C_9), 139.3 (C_3), 162.8 (C_1). $^{125}Te\{^1H\}$ NMR (CD_3CN, 25 °C, versus Me_2Te): (δ, ppm): 753.8. IR (KBr, ν_{max}/cm^{-1}): 3052 (m; $\nu_{C-H(aromatic)}$), 2922 (s; $\nu_{C-H(aliphatic)}$), 1178 (m; ν_{C-N}), 742 (m; $\nu_{C-H(aromatic)}$).

3. Results and discussion

Scheme 1 summarizes the syntheses of palladium(II) complexes **1–6**. The counter anion in complex **3** is ClO_4^-. A complex species having cation identical to that of **3** and anion PF_6^- has been reported earlier [14]. Earlier single crystals of **6** synthesized [14] in CH_3OH by reacting Na_2PdCl_4 with **L6** were grown from chloroform–hexane mixture (2:1). However, it has been prepared now by reacting $PdCl_2$ with **L6** in CH_3CN and its single crystals have been grown from $CH_3CN–CH_3OH$ mixture (3:2). The ^1H and $^{13}C\{^1H\}$ NMR spectra of presently synthesized **3** or **6** are only marginally different from those reported earlier [14] for species having cations similar to theirs. However, crystal data of these species differ from those reported earlier for complexes having similar cations. The difference in anion and/or absence of solvent molecule may be responsible for it. The earlier reported complexes containing cations corresponding to **3** or **6** crystallize with at least one $CHCl_3$ molecule and the complex corresponding to **3** has 0.5 H_2O additionally.

The molar conductance values in acetonitrile indicate 1:1 electrolyte nature of all complexes **1–6**. The complexes show good solubility in CH_3OH, CH_3CN, CH_2Cl_2 and $CHCl_3$. In diethyl and petroleum ether the complexes **1–6** were found to be nearly insoluble. The solutions of all complexes in DMSO showed signs of decomposition within few hours.

3.1. NMR and IR spectra

The ^1H and $^{13}C\{^1H\}$ NMR spectra of complexes **1–6** have been found characteristic of their molecular structures and support the presence of ligands **L1–L6** in them. The $^{77}Se\{^1H\}$ and $^{125}Te\{^1H\}$ NMR spectra of **2**, **3**, **5**, and **6** are given in supplementary material (Figs. S1–S4). The signals in $^{77}Se\{^1H\}$ NMR spectra of **2** and **5** appear shifted to higher frequencies by 177.9 and 164.5 ppm with respect to those of free **L2** and **L5**, respectively [22], as Se is coordinated to palladium centre. Similarly in $^{125}Te\{^1H\}$ NMR spectra of **3** and **6** the signals appear at frequencies higher by 353.9 and 339.5 ppm relative to those of free **L3** and **L6**, respectively [22], which are coordinated to palladium through Te. In ^1H and $^{13}C\{^1H\}$ NMR spectra of **1–6** signals generally appear at higher frequency relative to those of corresponding free ligand from **L1 to L6** [22], which coordinate with palladium in a tridentate mode. However, magnitude of shift to higher frequency is high for C_5–C_7 (up to 11.7 ppm in $^{13}C\{^1H\}$ NMR) and protons attached to them (up to 1.36 ppm in ^1H NMR) [22]. The signals of SCH_3 in $^{13}C\{^1H\}$ and ^1H NMR spectra of **1–6** also appear at higher frequency (up to 11.1 and 0.54 ppm, respectively) relative to those of appropriate ligands [22]. The signals of NH in ^1H NMR spectra of **4–6** appear at higher frequencies (up to 0.29 ppm) with respect to those of corresponding free ligand (from **L4 to L6**) [22].

The bands between 1585 and 1637 cm^{-1} in IR spectra of **L1–L3** are due to >C=N stretching. The C–N stretching in case of **L4–L6** appears from 1184 to 1191 cm^{-1} [22]. On complex formation both these IR bands show red shift (8–10 cm^{-1}) as N is coordinated with palladium.

3.2. Crystal structures

The crystal structures of **1**–**6** have been solved and their crystal data and refinements are given in Table S1. The ORTEP diagrams of representative cations i.e. of **2** and **5** are given in Figs. 1 and 2 with selected bond lengths and angles (more values are given in Supplementary material; Table S2). For ORTEP diagrams of cations of **1, 3, 4** and **6** see Supplementary material (Figs. S5–S8). The crystal structures of complexes having cations similar to those of **3** and **6** were solved earlier in orthorhombic and triclinic crystal system, respectively [14]. However crystal structures of **3** and **6** have been reported here in monoclinic crystal system. The unit cell parameters (Table S1 in Supplementary material) reveal that complexes **1** and **4** are iso-structural and same is true for **3** and **6**. However, complex **5** is not iso-structural with **2** but with **4**. The geometry around Pd in the cations of **1**–**6** is nearly square planar and the ligands are coordinated with Pd in a tri-dentate (S, N, E) (where E = S or Se or Te) mode forming six- and five-membered rings. The Pd–S bond lengths of **1–6**, 2.2707(10)–2.345(2) Å and Pd–Se bond lengths of **2** and **5** (2.4065(6) and 2.4045(16) Å, respectively) are in expected normal ranges [6,7,14,24]. The Pd–Te bond lengths of **3** (2.5307(13) Å) and **6** (2.5052(9) Å) are in normal range [7,14,25,26]. The greater flexibility of skeleton of **L6** than that of **L3** (due to reduction of >C=N) gives more room to sterically demanding Te, resulting in a somewhat stronger bond with Pd and shorter Pd–Te distance. Small differences in bond distances

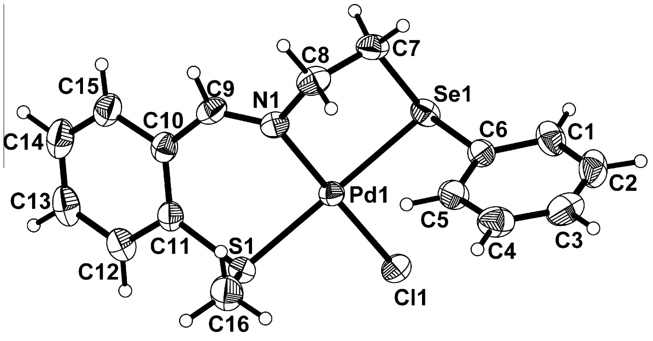

Fig. 1. ORTEP diagram of the cation of **2** with ellipsoids at the 30% probability level. The PF_6^- anion has been omitted for clarity. Selected bond lengths (Å): Pd(1)–Se(1) 2.4065(6), Pd(1)–S(1) 2.2864(12), Pd(1)–N(1) 2.012(3), Pd(1)–Cl(1) 2.2680(12); bond angles (°): Se(1)–Pd(1)–S(1) 178.52(3), Se(1)–Pd(1)–Cl(1) 91.96(4), Se(1)–Pd(1)–N(1) 87.01(10), S(1)–Pd(1)–Cl(1) 89.10(4), S(1)–Pd(1)–N(1) 91.96(11), N(1)–Pd(1)–Cl(1) 177.98(10). Symmetry transformation used to generate equivalent atoms: (i) *x*, *y*, *z*; (ii) −*x*, 0.5 + *y*, 0.5 − *z*; (iii) −*x*, −*y*, −*z*; (iv) *x*, 0.5 − *y*, 0.5 + *z*.

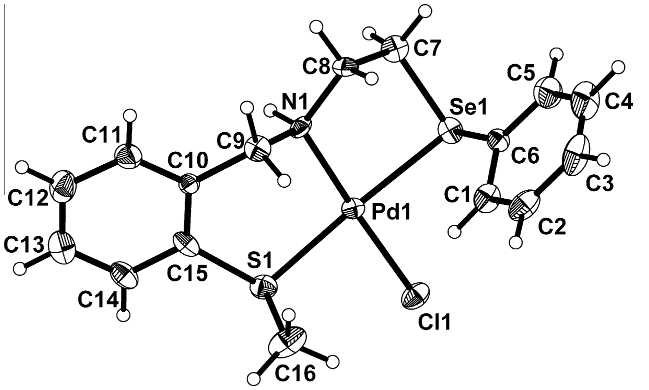

Fig. 2. ORTEP diagram of the cation of **5** with ellipsoids at the 30% probability level. The PF_6^- anion has been omitted for clarity. Selected bond lengths (Å): Pd(1)–Se(1) 2.4045(16), Pd(1)–S(1) 2.292(4), Pd(1)–N(1) 2.056(9), Pd(1)–Cl(1) 2.292(3); bond angles (°): Se(1)–Pd(1)–S(1) 177.22(10), Se(1)–Pd(1)–Cl(1) 90.09(10), Se(1)–Pd(1)–N(1) 87.04(3), S(1)–Pd(1)–Cl(1) 87.26(13), S(1)–Pd(1)–N(1) 95.2(3), N(1)–Pd(1)–Cl(1) 177.5(3). Symmetry transformation used to generate equivalent atoms: (i) *x*, *y*, *z*; (ii) −*x*, 0.5 + *y*, 0.5−*z*; (iii) −*x*, −*y*, −*z*; (iv) *x*, 0.5 − *y*, 0.5 + *z*.

arise due to variation in dentate character of ligands and their steric compulsions. The Pd−N and Pd−Cl bond lengths of complexes **1**–**6**, 2.012(3)–2.096(7) and 2.2680(12)–2.3056(11) Å, respectively are also normal. The bond angles at the coordinating S/Se/Te and N atoms are as expected for nearly trigonal-pyramidal and tetrahedral geometries, respectively.

3.3. Secondary interactions

In the crystals of **1**–**6**, due to non-covalent interactions several structural patterns have been observed. Some inter atomic distances for these interactions are given in Table S3 and they are shown in Figs. S9–S43 of Supplementary material. The P–F···H interactions are in the range 2.330(5)–2.870(6) Å and each PF_6^- is caged between complex cations (for example, see Fig. S9 for **1**). The intermolecular Cl···H interactions [2.995(1)–3.021(2) Å] result in chain type patterns. Fig. S12 in Supplementary material depicts it for **2**. The Cl–O···H interactions (2.413(20)–2.567(15) Å) result in a ring type of pattern as shown in *Fig.* S13 for **3**. In crystals of **4**, there are inter-molecular N–H···Cl–Pd interaction [2.671(44) Å] (*Fig.* S17). The ^-O_3Cl–O···H–C and N–H···ClO_4^-/^-O_3Cl–O···H–N interactions (See Figs. S13, S14, S20 and S21 in Supplementary material) exist in the crystals of **3** and **6**, respectively. In **1, 4** and **5**, one-dimensional chain structures are formed along *b*-axis by C–H···π interactions, which further assemble into two-dimensional (2D) sheet structure through P–F···H interactions (Figs. S23, S24, S29–S32). Further, these C–H···π interaction [2.785(1), 2.827(0) and 2.798(1) Å, respectively for **1**, **4** and **5**] patterns are almost similar as the three complexes are iso-structural. In **2** 1D chain structure formed along *b*-axis by C–H···π interactions further assembles into 2D sheet structure through P–F···H interactions (Figs. S25 and S26) but in a way different from those of **1**, **4** and **5**. In both **3** and **6**, there are C–H···π interactions but they do not become pivotal for any chain structure (Figs. S27, S28, S33 and S34). In **2**, Pd–Cl···N interactions form 1D chain structure along *c*-axis (Fig. S35). The intra- and inter-molecular Pd–Cl···S interactions [distances in the ranges 3.470(9)–3.992(6) and 3.425(30)–3.833(8) Å for **3** and **6**, respectively] (Figs. S39 and S42) give 1D chain structures and cause stacking along *b*-axis.

4. Conclusions

The six cationic Pd(II) complexes of composition [PdCl(**L**)][X] [**L** = 2-$MeSC_6H_4CH{=}NCH_2CH_2E$–C_6H_4–4-R (**L1**–**L3**) and 2-$MeSC_6H_4CH_2$–$NHCH_2CH_2E$–C_6H_4–4-R (**L4**–**L6**) (where E = S or Se, R = H; E = Te, R = OCH_3); X = PF_6 or ClO_4] have been synthesized by the reactions of $PdCl_2$ in CH_3CN with **L1**–**L6** and characterized by IR and multi-nuclei NMR spectroscopy and single crystal X-ray crystallography. The interesting non-covalent interactions have been observed in the crystals of **1**–**6**. The PF_6^- is caged by cationic Pd(II) species. The C–H···π and P–F···H interactions together result into two-dimensional (2D) sheet structure in the crystals of **1, 4** and **5**.

Acknowledgements

Authors thank Council of Scientific and Industrial Research (CSIR) New Delhi (India) for the Project No. 01(2421)10/EMR-II and Department of Science and Technology (India) for partial financial assistance given to establish single crystal X-ray diffraction facility at IIT Delhi, New Delhi (India) under its FIST program. P.S. thanks University Grants Commission (India) for the award of Junior and Senior Research Fellowship.

Appendix A. Supplementary material

CCDC 798691, 798692, 798693, 798694, 798695 and 798696 contain the supplementary crystallographic data for complexes **1**–**6**, respectively. These data can be obtained free of charge from The Cambridge Crystallographic Data Centre via www.ccdc.cam.ac.uk/data_request/cif. Supplementary data associated with this article can be found, in the online version, at doi:10.1016/j.ica.2012.01.007.

References

[1] J.W. Faller, J. Parr, Organometallics 19 (2000) 1829.
[2] I.D. Kostas, F.J. Andreadaki, D.K. Demertzi, C. Prentjas, M.A. Demerpzas, Tetrahedron Lett. 46 (2005) 1967.
[3] R.B. Bedford, C.S.J. Cazin, M.B. Hursthouse, M.E. Light, K.J.P.S. Wimperis, J. Organomet. Chem. 633 (2001) 173.
[4] P.R. Kumar, S. Upreti, A.K. Singh, Polyhedron 27 (2008) 1610.
[5] I.D. Kostas, B.R. Steele, A. Terzis, S.V. Amosova, A.V. Martynov, N.A. Makhaeva, Eur. J. Inorg. Chem. (2006) 2642.
[6] A. Kumar, M. Agarwal, A.K. Singh, Polyhedron 27 (2008) 485.
[7] A. Kumar, M. Agarwal, A.K. Singh, J. Organomet. Chem. 693 (2008) 3533.
[8] A. Kumar, M. Agarwal, A.K. Singh, R.J. Butcher, Inorg. Chim. Acta 362 (2009) 3208.
[9] R. Ganguly, B. Sreenivasulu, J.J. Vittal, Coord. Chem. Rev. 252 (2008) 1027 (and references therein).
[10] L.L. Koh, J.D. Ranford, W.T. Robinson, J.O. Stevenson, A.L.C. Tan, D. Wu, Inorg. Chem. 35 (1996) 6466.
[11] (a) I. Correia, S. Marcão, K. Koci, I. Tomaz, P. Adão, T. Kiss, T. Jakusch, F. Avecilla, J.C. Pessoa, Eur. J. Inorg. Chem. (2011) 694;
A. Biswas, M.G.B. Drew, C.J. Gómez-García, A. Ghosh, Inorg. Chem. 49 (2010) 8155;
(c) V.M. Leovac, P. Bombicz, K.M. Szécsényi, M.D. Joksović, Aust. J. Chem. 60 (2007) 615;
(d) B. Sreenivasulu, M. Vetrichelvan, F. Zhao, S. Gao, J.J. Vittal, Eur. J. Inorg. Chem. (2005) 4635;
(e) G.J. Colpas, B.J. Hamstra, J.W. Kampf, V.L. Pecoraro, Inorg. Chem. 33 (1994) 4669;
(f) V.C. Gibson, C. Newton, C. Redshaw, G.A. Solan, A.J.P. White, D.J. Williams, Dalton Trans. (1999) 827.
[12] R.P. Kumar, A.K. Singh, R.J. Butcher, P. Sharma, R.A. Toscano, Eur. J. Inorg. Chem. (2004) 1107.
[13] P.R. Kumar, S. Upreti, A.K. Singh, Inorg. Chim. Acta 361 (2008) 1426.
[14] G.K. Rao, A. Kumar, J. Ahmed, A.K. Singh, Chem. Commun. 46 (2010) 5954.
[15] SADABS V2.10 (G.M. Sheldrick, 2003).
[16] (a) G.M. Sheldrick, Acta Crystallogr., Sect. A 46 (1990) 467.;
(b) G.M. Sheldrick, SHELXL-NT Version 6.12, University of Gottingen, Germany, 2000.
[17] A.R. Katritzky, Y.-J. Xu, H.-Y. He, S. Mehta, J. Org. Chem. 66 (2001) 5590.
[18] A. Khanna, A. Bala, B.L. Khandelwal, J. Organomet. Chem. 494 (1995) 199.
[19] A.K. Singh, V. Srivastava, Phosphorus Sulfur Silicon 47 (1990) 471.
[20] K.J. Irgolic, R.A. Zingaro, Reactions of organotellurium compounds, in: E. Becker, M. Tsutsui (Eds.), Organometallic Synthesis, Vol. 2, John Wiley and Sons, Inc., 1971.

[21] B.S. Furniss, A.J. Hannaford, P.W.G. Smith, A.R. Tatchell, Vogel's Textbook of Practical Organic Chemistry, fifth ed., ELBS, Longman Group UK Ltd., 1989.
[22] P. Singh, A.K. Singh, Organometallics 29 (2010) 6433.
[23] P. Singh, D. Das, M. Singh, A.K. Singh, Inorg. Chem. Commun. 13 (2010) 223.
[24] D. Das, G.K. Rao, A.K. Singh, Organometallics 28 (2009) 6054.
[25] G. Singh, A.K. Singh, P. Sharma, J.E. Drake, M.B. Hursthouse, M.E. Light, J. Organomet. Chem. 688 (2003) 20.
[26] A.K. Singh, J. Sooriyakumar, S. Husebye, K.W. Tornroos, J. Organomet. Chem. 612 (2000) 46.